Electronic Supplementary Material (ESI) for Integrative Biology.

Supplementary Information

Quantifying cell-induced matrix deformation in three dimensions based on imaging matrix fibers

Jacob Notbohm,[1†] Ayelet Lesman,[2†] David A. Tirrell,[2] Guruswami Ravichandran[1*]

[1]Division of Engineering and Applied Science, California Institute of Technology
[2]Division of Chemistry and Chemical Engineering, California Institute of Technology
Pasadena, CA, USA

[*]Correspondence to: ravi@caltech.edu.
[†]These authors contributed equally to this work.

Supplemental Note: Scaling of matrix fiber density over distance

In the experiments described in Fig. 3, a sphere is placed under compression within a fibrous matrix. The linear elastic solution for displacements within the matrix is given by Goodier [27], which shows radial displacements u_r are $u_r = Ar^{-2} + Br^{-4}$ where r is distance from the sphere and A and B are constants. For an axisymmetric geometry, normal strains in the radial and angular (hoop) directions are given by $\varepsilon_{rr} = \partial u_r/\partial r$ and $\varepsilon_{\theta\theta} = u_r/r$. Thus, for $r \gg 1$, both normal strain components scale as

$$\varepsilon_{rr}, \varepsilon_{\theta\theta} \sim r^{-3}. \tag{1}$$

If the fibrous matrix behaves as a linear elastic material, the strains can be related to the fluorescence intensity, and thus the scaling of fluorescence intensity with distance can be computed. In the compression experiment of Fig. 3, the matrix far from the sphere is under uniform strain in the z direction, ε_{zz}. Near the sphere, the matrix has strain tensor components in all three normal directions, $\varepsilon_{rr}, \varepsilon_{\theta\theta}, \varepsilon_{zz}$. Consider three different states of strain within the matrix. State 0 is a reference state that is completely free of strain and stress. State 1 represents the far field strain, with a normal strain component along the axial z direction given by $\varepsilon_{zz} = \varepsilon$ and all other components of the strain tensor equal to zero. State 2 represents the strain near the sphere with strain tensor components given by $\varepsilon_{zz} = \varepsilon$ and nonzero strain tensor components ε_{rr} and $\varepsilon_{\theta\theta}$. Assume fluorescence intensity is linearly proportional to fiber density ρ, which is inversely proportional to local volume V. From linear elasticity, the relative change in volume from a reference to a current state $(V_i - V_0)/V_0$ is equal to the trace of the strain tensor, with $i = 1, 2$ indicating states 1 and 2 respectively. Thus the equations relating change in volume to strain for states 1 and 2 are as follows:

$$\begin{aligned} \frac{V_1}{V_0} &= \varepsilon + 1 \\ \frac{V_2}{V_0} &= \varepsilon_{rr} + \varepsilon_{\theta\theta} + \varepsilon + 1. \end{aligned} \tag{2}$$

The change in fiber density from state 1 to state 2 represents the fluorescence intensity due to the rigid sphere in the fibrin matrix under uniform compresion:

$$\frac{\rho_2}{\rho_1} = \frac{1}{1 + \frac{1}{1+\varepsilon}(\varepsilon_{rr} + \varepsilon_{\theta\theta})}. \tag{3}$$

Assuming small strains, expand the $(1+\varepsilon)^{-1}$ term and ignore terms of order ε^2 and larger. This gives

$$\frac{\rho_2}{\rho_1} = \frac{1}{1 + \varepsilon_{rr} + \varepsilon_{\theta\theta}}. \tag{4}$$

Combining with Eq. 1 gives the scaling of matrix fiber density over distance,

$$\frac{\rho_2}{\rho_1} = \frac{1}{1 + Cr^{-3}}, \tag{5}$$

where C is a constant. For intermediate values of r, the curves in Fig. 3d match the scaling of Eq. 5 well, and as r gets large, the ratio ρ_2/ρ_1 approaches unity, also in agreement with Fig. 3d.

Supplemental Figures

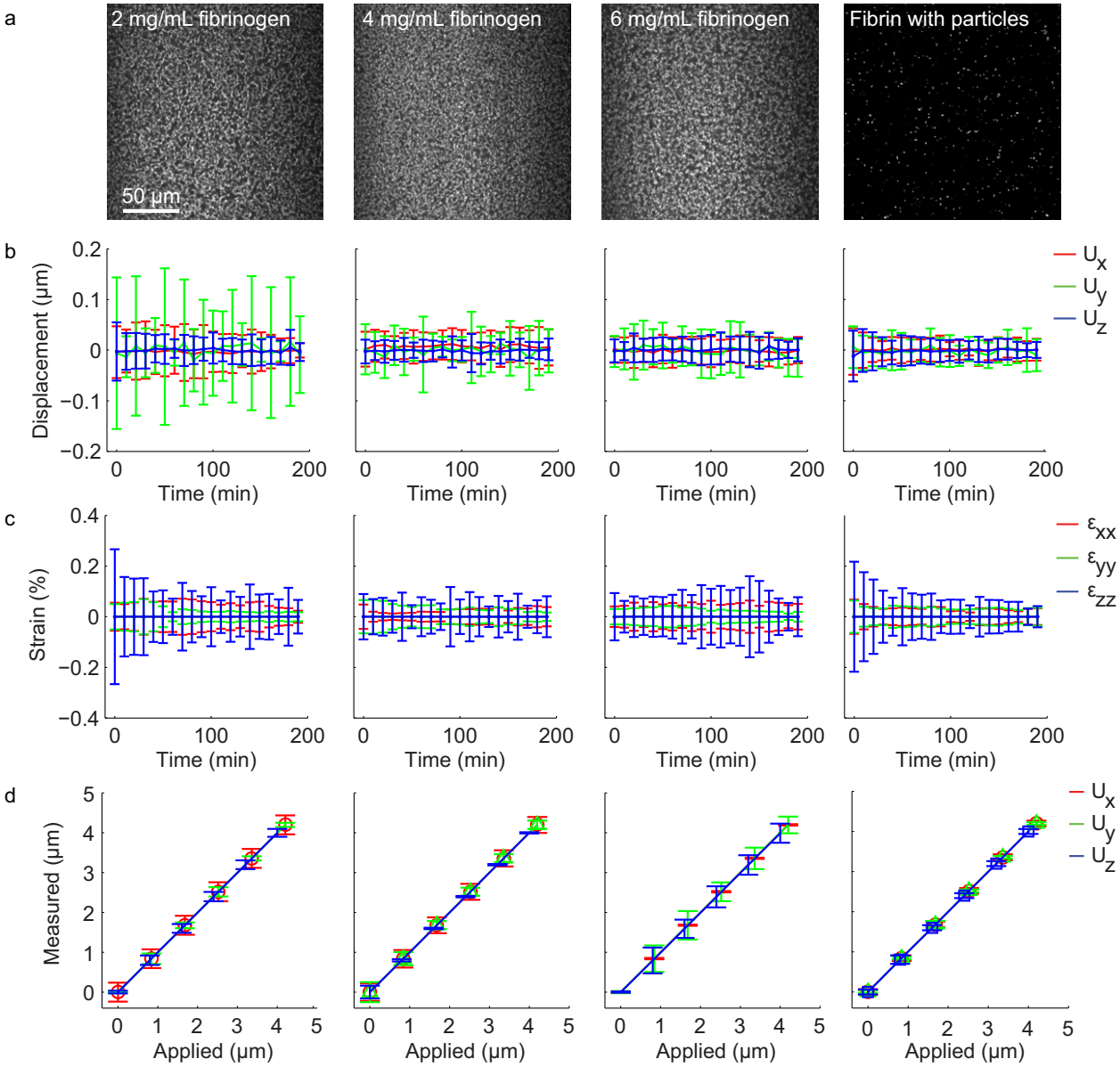

Figure S1: The DVC technique successfully measures displacements and strains within a variety of fibrin network densities. (a) Fluorescently labeled fibrin gels are made with fibrinogen concentrations of 2–6 mg/mL. For comparison, 1 µm fluorescent particles are encapsulated in fibrin gels in separate experiments. The noise floor for displacement measurement is quantified with cell-free control experiments. In these experiments, volume stacks of labeled fibrin matrix or fluorescent particles in fibrin are collected over time at four different positions. At the end of the time lapse 85 µM blebbistatin is added to capture a reference time point. Matrix displacements are then computed with DVC using this reference. (b) Typical errors due to noise in measuring displacements in all three spatial directions (U_x, U_y, U_z) are ∼0.05–0.1 µm. (c) Normal strain components (ε_{xx}, ε_{yy}, ε_{zz}) are computed from the displacements with a typical noise of ∼0.1–0.2% strain. Plots in (b) and

(c) show mean ± standard deviation for four different positions within the matrix after correcting for volumetric strains as described in the methods. (d) The accuracy of the DVC method is assessed by applying computational translations of up to 5 µm to the image stacks of the fibrin matrix in all three spatial directions (U_x, U_y, U_z) and then correlating using DVC. For all concentrations of fibrinogen, the DVC accurately measures the applied displacements with typical errors of 1–5%.

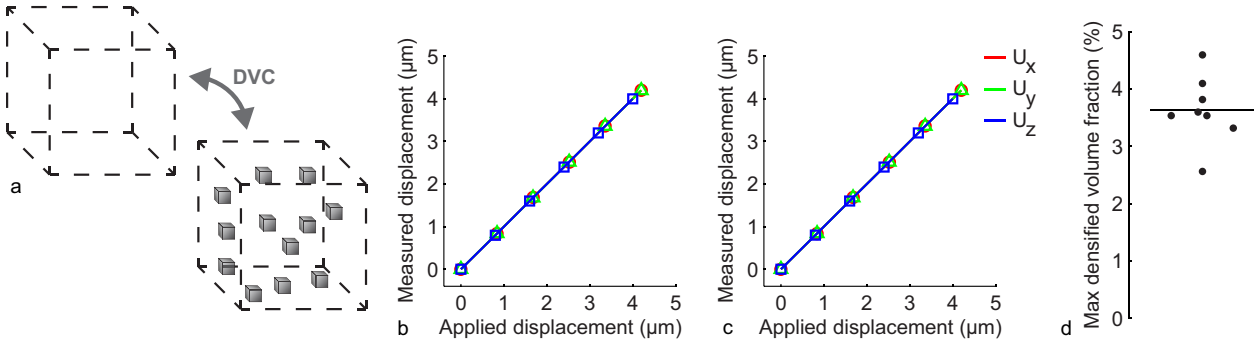

Figure S2: To consider the effect of fiber densification and degradation on the displacement measurement, further tests of the DVC's accuracy were conducted. (a) A 64×64×64 voxel subvolume of native matrix was degraded by adding 12 cubic spots, each having a size of 9×9×9 voxels and an intensity equal to the brightness of the 99th percentile of all voxels within the subvolume. These 12 spots had a volume equal to 3% of the subvolume. (b) Computational translations were applied to the subvolume in all three spatial directions (U_x, U_y, U_z), and displacements were subsequently measured with DVC. (c) The analysis was repeated using 12 holes (with zero fluorescence intensity), representing degraded regions within the matrix. Results for both bright spots (densification, b) and holes (degradation, c) show that the displacement measured with DVC matches the applied displacement with error equal to the noise floor of the DVC (Supplemental Fig. S1b). (d) Maximal volume fraction of cell-induced fiber densification within a DVC subvolume is quantified by measuring the volume of an isosurface of the matrix (see methods for more information). For 8 different cells, the maximal volume fraction averages 3.6%, which closely matches the 3% limit for accuracy of the DVC.

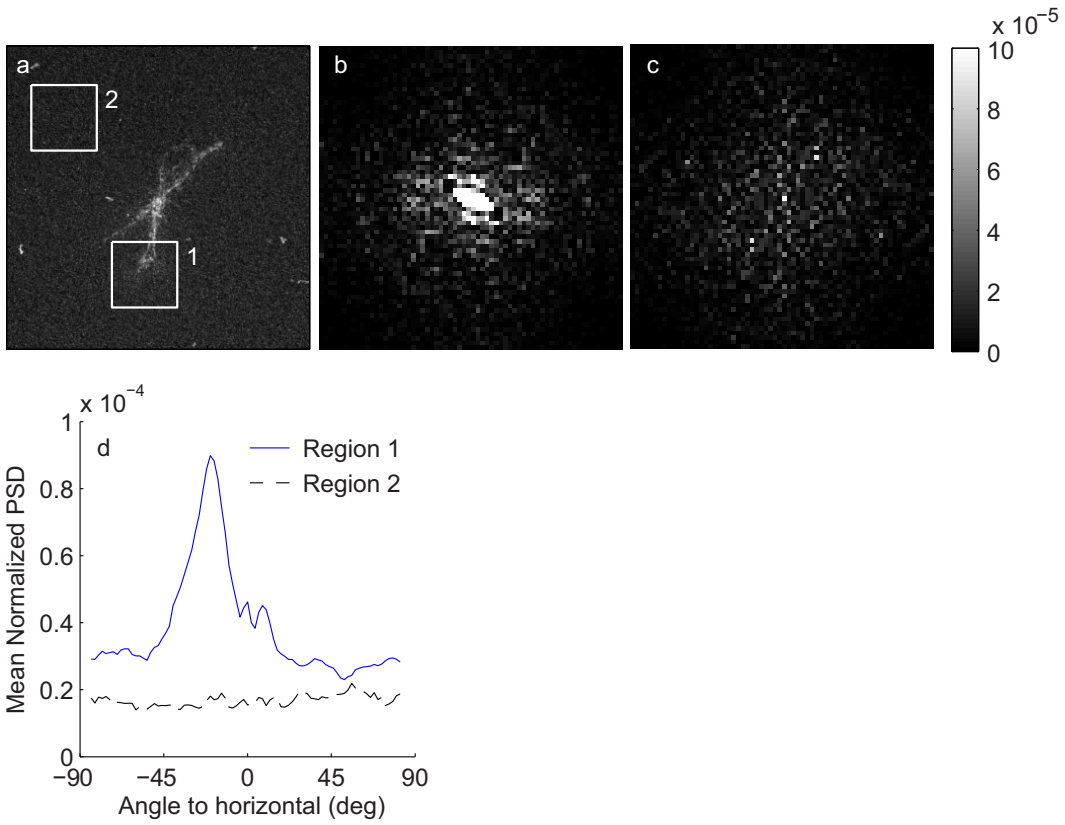

Figure S3: Cell-induced matrix alignment was characterized by the power spectral density (PSD), as described in the methods. (a) The maximum intensity projection of a volume stack of matrix fibers was used for analysis. Two regions (labeled 1 and 2) were selected, and the PSD was computed for each region (plotted in panels b, and c, respectively). Fiber alignment is identified by bands in the PSD; these bands are oriented at an angle of 90° to the orientation of fiber alignment. (d) Mean values of the PSD were computed along lines drawn from the center to the edge of the PSD image for various angles to the horizontal. Thus, the peak at an angle of –20° indicates fiber alignment at an angle of 70° for region 1.

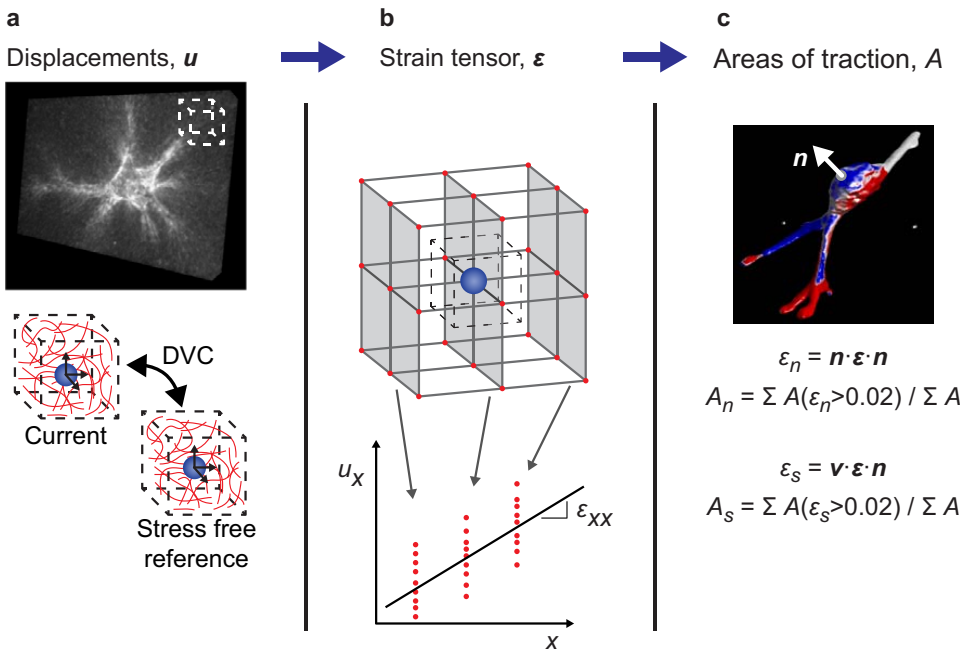

Figure S4: Summary of the technique for computing displacements and strains. (a) 3D matrix displacements are computed throughout the volume by using DVC. The DVC divides the entire volume stack of matrix fibers into small subsets, each having a unique distribution of fluorescence intensity. It then correlates each subset to a reference, stress-free condition to calculate displacements in the matrix. (b) The strain tensor throughout the matrix is then computed by fitting a 3×3×3 grid of points around the point of interest to a 3D linear function and taking derivatives in the x, y, and z directions. An example of this computation is shown for ε_{xx}, the normal strain in the x direction. Red dots represent the 3×3×3 grid of points used for numerical differentiation. (c) Areas of the cell applying normal and shearing forces to the matrix are computed from the matrix strain tensor near the cell body. Normal and shearing components of the strain tensor are computed as described in the methods, and relative areas of the cell exhibiting normal and shearing forces are computed.